OPTICA

Dual-frequency-comb UV spectroscopy with one million resolved comb lines

Andrey Muraviev,[1] Dmitrii Konnov,[1] Sergey Vasilyev,[2] and Konstantin L. Vodopyanov[1,*]

[1]CREOL, the College of Optics and Photonics, University of Central Florida, Orlando, Florida 32816, USA
[2]IPG Photonics Corporation, Marlborough, Massachusetts 01752, USA
*vodopyanov@creol.ucf.edu

Received 8 August 2024; revised 18 September 2024; accepted 18 September 2024; published 31 October 2024

We present high-resolution dual-comb spectroscopy across two broad UV spectral regions spanning 372–410 nm and 325–342 nm. This is achieved by generating sixth and seventh harmonics, respectively, from a low-noise 2.35 μm Cr:ZnS dual-comb laser system. The sixth harmonic band contains approximately 1,000,000 spectrally resolved comb lines, while the seventh harmonic band—around 550,000 comb lines. With the line spacing of 80 MHz, this corresponds to a resolving power of up to 10 million, offering remarkable spectral resolution.

https://doi.org/10.1364/OPTICA.536971

High-resolution ultraviolet (UV) spectroscopy offers unique insights into electronic transitions in atoms and molecules, making it highly desirable for a wide range of applications. These include testing fundamental laws of physics, chemical analysis, photochemistry, trace gas sensing in the atmosphere, and exoplanet exploration [1,2]. A cutting-edge frontier in UV spectroscopy is the study of the unique isomeric transition in Thorium-229 nuclei, occurring at a wavelength of 148.3 nm [3,4].

The resolution of grating spectrometers in the UV regime is limited to about 100 GHz while the best Fourier transform spectrometers allow to achieve 15 GHz resolution [5]. Conversely, dual-comb spectroscopy (DCS) [6,7] features simultaneously broad spectral coverage, rapid data acquisition, and superior spectral resolution ultimately limited by the linewidth of a comb mode (Hz to kHz range). Another advantage of DCS is a straightforward calibration of the frequency scale with the accuracy and precision of an atomic clock.

The key requirement and the main challenge of the DCS method is the necessity to maintain two optical comb sources in robust phase lock for an extended time with the mutual timing jitter $\ll 1/\nu$ where ν is the optical frequency. This condition, in turn, allows to resolve individual comb modes and, hence, enables DCS with the highest performance. A detailed analysis [8] shows that even at the ideal phase lock, the performance of DCS is still limited by the optical power per comb mode and by the comb's relative intensity noise (RIN). The main trade-off in the DCS method is the scaling of the spectral signal-to-noise ratio (SNR) as $\propto \sqrt{\tau}/M$, where τ is the coherent averaging time and M is the number of comb modes resolved with a single detector. Thus, the wider the DCS bandwidth, the more stringent the comb noise level requirements must be to keep the data acquisition time at a reasonable level.

The DCS technique is now well established across the visible to THz spectral range. Hundreds of thousands of comb modes spanning about an optical octave can be measured with high speed (up to video rate) and with high dynamic range (up to 50 dB) [9–11]. However, research on the UV DCS is still in its early stages and remains relatively limited. The challenges are caused by a combination of several factors. Currently, UV combs are produced through a harmonic generation process, which results in the increase of intensity and phase noise—with quadratic dependence of the noise power spectral density on the harmonic order [12]. Further, high optical frequencies of UV combs (≈ 1 PHz) impose tighter constraints on the mutual timing jitter ($\ll 1$ fs).

Consequently, the current demonstrations of DCS in the UV lack either resolution, or bandwidth, or both. McCauley *et al.* [13] demonstrated DCS in the deep UV region at wavelengths near 262 nm. The combs were produced by quadrupling the frequency of Yb-fiber (1030 nm) lasers. DCS with an instantaneous spectral span of 2 THz was achieved with high, 1.2 GHz, resolution, albeit the comb modes were not resolved. Fürst *et al*. [14] produced broadband UV combs that span 334–354 nm (frequency extent 50.3 THz) using the third harmonic of Yb-fiber lasers with subsequent nonlinear spectral broadening via self-phase modulation in a silica fiber, with the DCS resolution limited to 50 GHz. Di *et al*. [15] demonstrated DCS with optical harmonics (up to ninth) of a dual-comb mid-IR system operating at $\lambda = 3.6$ μm. The comb-mode-resolved spectra with circa 10 THz bandwidth were obtained for up to the eighth harmonic, which corresponds to the visible wavelength of 450 nm. However, the signal at the ninth harmonic (UV range) was too weak and too noisy to perform DCS. The only two demonstrations of comb-line-resolved DCS in the UV reported to date are based on frequency quadrupling of 1550 nm comb sources to access the wavelengths near 390 nm. Xu *et al*. [16] used two inherently coherent electro-optic combs generated from an amplified narrow-linewidth semiconductor laser and a photon-counting method to resolve 100 and 130 comb modes spaced by 500 and 200 MHz, respectively. Chang *et al*. [17], used mutually phase locked femtosecond Er-fiber oscillators and reported 30,000 resolved comb modes (frequency extent

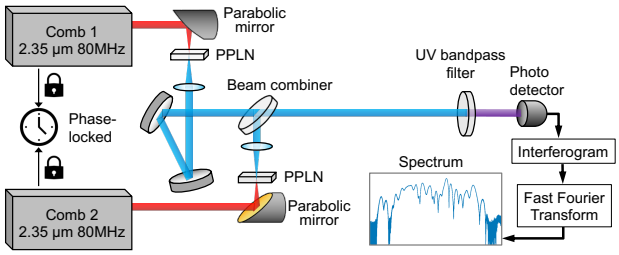

Fig. 1. Schematic of the DCS laser setup.

3 THz) at 100 MHz spacing. The authors used a high-dynamic servo control to achieve mutual phase coherence between the two combs and post-processed the acquired time-domain data streams using self-correction algorithms. To date, this is the highest number of spectrally resolved comb lines achieved in the UV.

Here, using a new laser platform as a driving source, we perform dual-comb laser spectroscopy in two ultra-wide (frequency span up to 80 THz) UV spectral bands: 325–342 nm and 372–410 nm and simultaneously resolve ∼550,000 and ∼1,000,000 comb lines spaced by 80 MHz, respectively.

The front end of our setup (Fig. 1) is a dual-comb system based on a pair of robustly phase-locked ultrafast Cr:ZnS lasers referenced to a Rb clock, similar to [18,19]. The Cr:ZnS comb source is arranged as a master oscillator–power amplifier system at the center wavelength 2350 nm, 3 Watt output power, and 25 fs pulse duration. The Cr^{2+} : ZnS gain elements are optically pumped at 1567 nm by an Er-doped fiber laser system. The pulse repetition rate (f_{rep}) and, hence, the mode spacing of the comb is 80 MHz. The spectral span of the pump laser comb is 60 THz ($\Delta\lambda = 1170$ nm) at −10 dB level, which corresponds to 3/4 million comb modes with the power per mode as high at 10 μW near the peak and 1 μW at the 10 dB wings of the spectrum.

An important feature of Cr:ZnS-based comb sources is their inherent low intensity and phase noise. This is attributed to the instantaneous nonlinear losses due to the randomly quasi-phase matched second harmonic generation in the gain medium (for both oscillator and amplifier) serving as a noise eater [20,21]. Preliminary measurements show that modes of a free-running Cr:ZnS comb have rather narrow linewidths of about 12 kHz in 0.4 ms, which greatly simplifies the comb's referencing and stabilization.

The comb's referencing includes the locking of its carrier-envelope offset frequency f_0 and of its mode spacing f_{rep}. The f_0 is measured as a beatnote between the comb's third and fourth harmonics at ≈ 650 nm and then locked by modulating the laser oscillator pump. The second harmonic of the comb is heterodyned with a narrow-linewidth single frequency reference laser at 1064 nm and the beatnote is locked by adjusting the laser cavity length, thus locking the mode spacing f_{rep}. The timing jitter of the 2350 nm comb with respect to the reference laser is <0.1 fs and its RIN is typically below 0.1% level (10 Hz to 40 MHz range). Thus, the Cr:ZnS comb source combines broad spectrum and high power per comb mode with ultra-low noise—a set of parameters that is beneficial for a high-performance DCS. Further, MW-level peak power of the comb facilitates efficient up-conversion to the UV range, as described below.

For the nonlinear frequency conversion, the pump mid-IR comb is coupled to a bulk periodically poled lithium niobate crystal (PPLN). The PPLN chip with the total length 0.5 mm includes three consecutive sections with the poling periods 33.6, 13.8, and

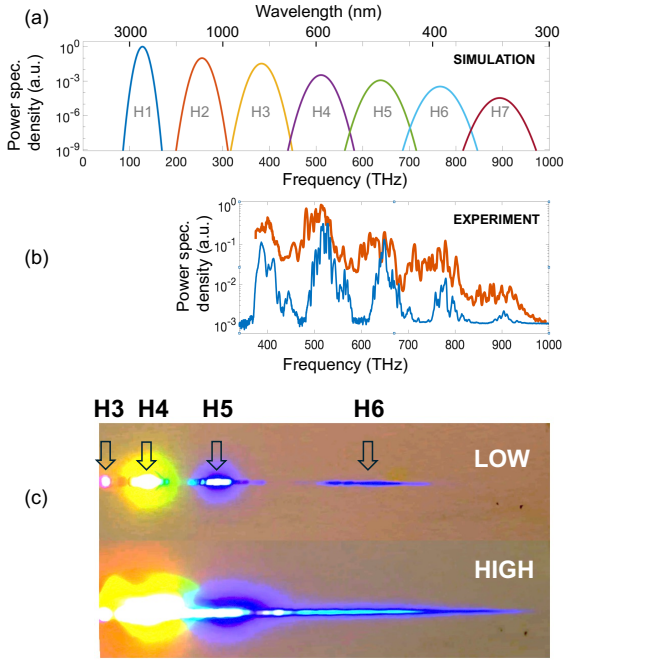

Fig. 2. (a) Harmonic spectra based on the measured laser spectrum (H1) and the simulations assuming a perturbative phase-matched regime (H2–H7). (b) The measured low-resolution H3–H7 spectra obtained with a UV-VIS spectrometer in two regimes: at low (900 mW) laser pump power (blue curve) and high (3 W) pump power (red curve). (c) Screen patterns (H3–H6) obtained by dispersing the harmonics' spectrum with a prism.

12.8 μm designed for cascaded generation of the second, third, and fourth harmonics from the 2350 nm input, correspondingly. The higher harmonics, up to seventh order, were also generated and, surprisingly, had enough power for DCS interferograms to be detected in real time. Developing a theoretical framework to describe this effect is an ongoing study. Figure 2(a) shows the harmonic spectra based on the measured laser spectrum (H1) and the simulations assuming a perturbative phase-matched regime (H2–H7), which serve as a trace for the eye. The average power level of the generated harmonic combs was measured to be: 300 mW–100 mW–10 mW–3.5 mW–1 mW–0.1 mW for harmonics H2–H7, respectively.

The measured harmonics' spectra are shown in Figs. 2(b) and 2(c). Here we observed how the spectral peaks of the high-order harmonics merge as the pump laser power increases from 900 mW ("low") to 3 W ("high"). The spectra of Fig. 2(b) were acquired using a low-resolution UV-VIS spectrometer from Ocean Optics (model QP200-2-SR-BW), sensitive to H3–H7, and the screen patterns of Fig. 2(c)—by dispersing the spectrum on a screen using a BK7 glass prism (the photo camera was only sensitive to H3–H6). The fusion of harmonics of different orders to a single continuum was confirmed, similar to [22], by detecting the beats between any pair of harmonics in the regions of their spectral overlap (including H6 and H7) that occur at the offset frequency of the driving laser f_0. It is worth noting that creating a carrier-envelope-phase (CEP) stable Cr:ZnS pump comb ($f_0 = 0$), as described, for example, in [23], may allow producing a single CEP-stable mid-IR-to-UV optical frequency comb with ∼ 1 PHz bandwidth.

The DCS was performed by combining two combs with the same harmonic order n using a 50/50 beam combiner and a fast

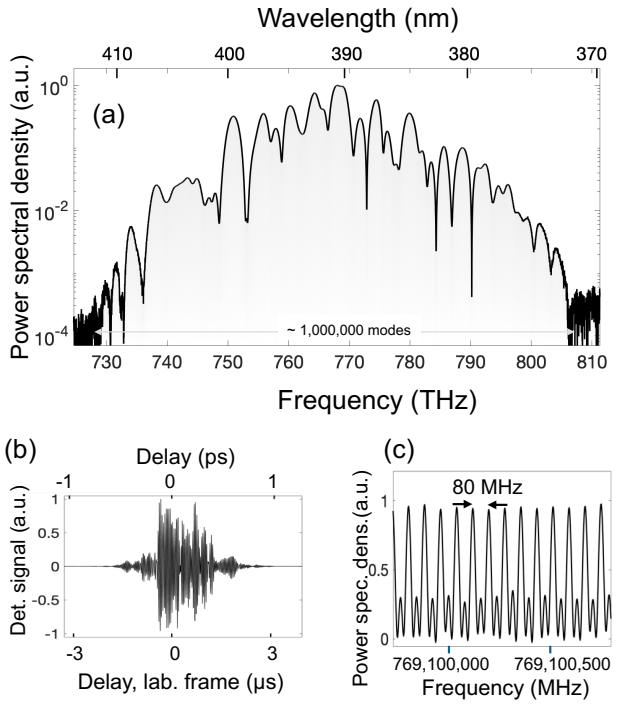

Fig. 3. (a) Spectrum of H6 containing close to a million comb lines. (b) The averaged IGM centerburst. (c) Portion of the comb-line-resolved spectrum.

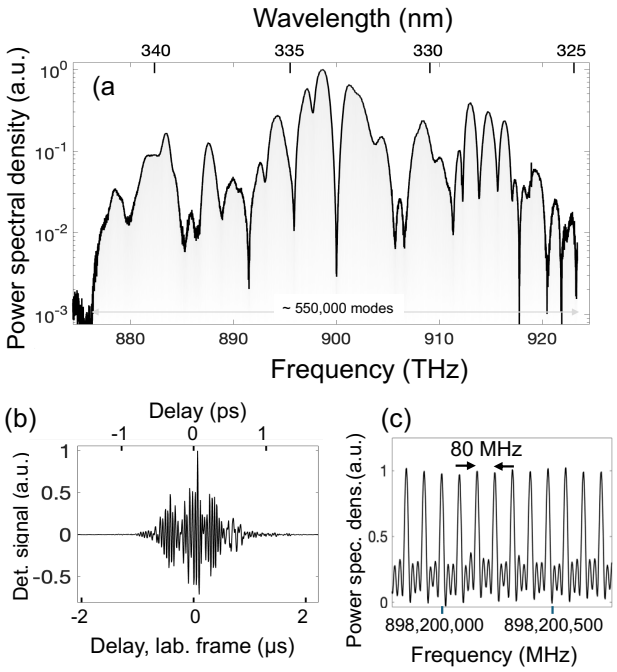

Fig. 4. (a) Spectrum of H7. (b) The corresponding IGM centerburst. (c) Portion of the comb-line-resolved spectrum.

(>50 MHz) photodetector. For the whole set of generated harmonics, H1–H7, we were able to observe comb-mode-resolved spectra.

Figure 3(a) shows the log-scale DCS spectrum of H6 obtained using an avalanche silicon detector. The repetition rate offset between the two combs was $\Delta f_{\mathrm{rep}} = 25.8$ Hz and we used coherent averaging of $N = 6 \times 10^5$ full-range single interferograms (IGMs) with an averaging time of $\tau = 387$ min. No apodization or post-processing of the raw data before Fourier transform was used. For each IGM, the data acquisition process was triggered using an oscilloscope, by a sharp edge of the IGM. This can be regarded as an elementary phase correction, similar to [24]. The averaged IGM centerburst is shown in Fig. 3(b). The H6 wavelength span is 372.5–410.3 nm (spectral width 74 THz) at −30 dB level, corresponding to 928,000 comb lines, while at the noise level (−40 dB) the bandwidth is 80 THz containing one million comb lines. For the signal-to-noise ratio for this spectrum of SNR = 588 and the number of modes M = 928,000, this results in a record high DCS figure of merit (FOM), defined in [7], of $M \times \mathrm{SNR}/\sqrt{\tau} = 3.6 \times 10^6\ \mathrm{Hz}^{1/2}$.

To resolve the comb structure of H6, we coherently averaged $N = 2 \times 10^4$ waveforms, each consisting of four consecutive IGMs. A close-up view of the corresponding comb-line-resolved spectrum with the finesse of four, corresponding to the number of consecutive IGMs recorded, is shown in Fig. 3(c).

A log-scale spectrum of H7 is shown in Fig. 4(a) and is derived from $N = 3 \times 10^5$ coherently averaged single IGMs ($\Delta f_{\mathrm{rep}} = 62.5$ Hz, $\tau = 80$ min). The span is 325.4–341.8 nm (spectral width 44 THz) at −30 dB level, corresponding to 550,000 comb lines and the DCS FOM $= 7.1 \times 10^5\ \mathrm{Hz}^{1/2}$. The IGM centerburst is shown in Fig. 4(b), and the comb-line-resolved spectrum, where we coherently averaged $N = 2 \times 10^4$ waveforms consisting of four consecutive IGMs, in Fig. 4(c). In this spectral range, the 80 MHz comb-line spacing corresponds to the wavelength resolution $\Delta\lambda = 30$ fm and the resolving power $\lambda/\Delta\lambda = 1.1 \times 10^7$. The noticeable intensity variations in the H7 spectrum are likely caused by interferences of multiple paths in the process of high-harmonic generation—in the sense that 7ω can be produced via $3\omega + 3\omega + \omega$, $3\omega + 4\omega$, or $2\omega + 2\omega + 2\omega + \omega$, etc., processes. We note that in the case of broadband molecular spectroscopy, the "zeros" in the spectrum can be shifted by tilting PPLN crystals.

As a spectroscopy demonstration, we measured the reflection spectrum of a volume Bragg grating (BragGrate Mirror from IPG/OptiGrate) with a narrow (finesse > 4000) reflection band at 406 nm, tuned to 390 nm (the center of the H6 spectrum) by tilting the grating, mounted on a rotation stage, by ∼22 deg from the normal incidence. The average power in the reflected beam was approximately 5 μW. Figure 5(a) shows the log-scale reflection spectrum with the incoming spectrum in the background for reference. Here we used $\Delta f_{\mathrm{rep}} = 3.05$ kHz and coherently averaged a single IGM for only 1 s [the centerburst is shown in Fig. 5(b)]. Figure 5(c) shows a close-up view of the spectrum with a width of 200 GHz (2500 comb lines) at −10 dB level. The sharp increase in SNR here occurs due to the reduction in the number of comb lines, in full agreement with [7]. In addition, a narrow spectrum allows to increase the rate of data acquisition via increasing Δ_{frep}.

Narrowing the spectral window also allowed us to refine the UV comb structure. By recording a 1 s long stream of 3050 consecutive IGMs without any further data processing, we measured a comb-line-resolved spectrum of H6 with the finesse as high as 2600 [a close-up view of the spectrum is shown in Fig. 5(d)]. The full width at half maximum (FWHM) of a comb line [inset to Fig. 5(d)] is 1.17 Hz in the RF domain (30.8 kHz optical). It is slightly (17%) above the Fourier limit for the 1 s record time and this small discrepancy can be explained by a mutual timing jitter between the two combs, which in our case was estimated to be 0.3–0.4 fs (rms)—through superimposing, with a fixed time delay,

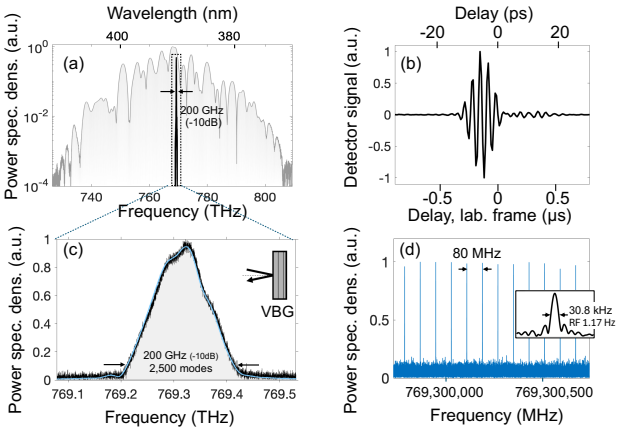

Fig. 5. (a) Reflected spectrum from the volume Bragg grating (black curve) and the input spectrum (gray filled curve). (b) The IGM centerburst for the reflected spectrum. (c) A close-up view of the reflected spectrum for 1 s averaging (black curve) and 246 s averaging (blue curve). (d) A close-up view of the comb-mode-resolved spectrum obtained from a 1 s stream of data. The inset shows the shape of a single comb line. VBG, volume Bragg grating.

successive IGMs from a long data record. One should note that this narrow 200 GHz band can be selected anywhere within the entire H6 spectrum—by simply varying the incidence angle on the volume Bragg grating within 0...35°.

In conclusion, to the best of our knowledge, this is the first demonstration of ultra-wideband dual-comb spectroscopy in the UV range, capable of simultaneously resolving up to one million comb lines, all referenced to an atomic clock. With a resolving power of 10^7 and a record DCS figure of merit reaching 3.6×10^6 Hz$^{1/2}$, this system sets a new benchmark in the UV. In fact, given the narrow comb lines, the spectral resolution can be made much better than the comb-line spacing via measurements with a gradually shifted comb offset [25]. While the PPLN transmission currently limits the UV region to wavelengths above 325 nm, non-perturbative high-harmonic generation in bulk crystals, such as ZnO or GaSe driven by mid-IR pulses, presents a promising pathway to accessing deeper UV regions, potentially down to $\lambda \approx 100$ nm [26,27]. This advancement could open doors to new areas of laser spectroscopy, such as the development of a nuclear clock based on the ^{229}Th isotope transition near 148 nm.

Funding. Air Force Office of Scientific Research (FA9550-23-1-0126); U.S. Department of Energy (BR #KA2601020).

Acknowledgment. We thank Vadim Smirnov (IPG Photonics Corp./OptiGrate) for providing volume Bragg grating samples.

Disclosures. The authors declare no conflicts of interest.

Data availability. Spectral data are available upon reasonable request.

REFERENCES

1. V. Schuster, C. Liu, R. Klas, *et al.*, Opt. Express **29**, 21859 (2021).
2. S. Galtier, C. Pivard, and P. Rairoux, Remote Sens. **12**, 3444 (2020).
3. J. Tiedau, M. V. Okhapkin, K. Zhang, *et al.*, Phys. Rev. Lett. **132**, 182501 (2024).
4. C. Zhang, T. Ooi, J. S. Higgins, *et al.*, Nature **633**, 63 (2024).
5. R. Gupta and S. G. Kaplan, J. Res. Natl. Inst. Stand. Technol. **108**, 429 (2003).
6. N. Picqué and T. W. Hänsch, Nat. Photonics **13**, 146 (2019).
7. Coddington, N. Newbury, and W. Swann, Optica **3**, 414 (2016).
8. N. R. Newbury, I. Coddington, and W. Swann, Opt. Express **18**, 7929 (2010).
9. J. Roy, J.-D. Deschênes, S. Potvin, *et al.*, Opt. Express **20**, 21932 (2012).
10. H. Timmers, A. Kowligy, A. Lind, *et al.*, Optica **5**, 727 (2018).
11. D. Konnov, D. Muraviev, S. Vasilyev, *et al.*, APL Photonics **8**, 110801 (2023).
12. C. Benko, T. K. Allison, A. Cingöz, *et al.*, Nat. Photonics **8**, 530 (2014).
13. J. J. McCauley, M. C. Phillips, R. R. D. Weeks, *et al.*, Optica **11**, 460 (2024).
14. L. Fürst, A. Kirchner, A. Eber, *et al.*, Optica **11**, 471 (2024).
15. Y. Di, Z. Zuo, D. Peng, *et al.*, Photonics Res. **11**, 1373 (2023).
16. A. Xu, Z. Chen, T. W. Hänsch, *et al.*, Nature **627**, 289 (2024).
17. K. F. Chang, D. M. B. Lesko, C. Mashburn, *et al.*, Opt. Lett. **49**, 1684 (2024).
18. S. Vasilyev, A. Muraviev, D. Konnov, *et al.*, Opt. Lett. **48**, 2273 (2023).
19. S. Vasilyev, V. Smolski, J. Peppers, *et al.*, Opt. Express **27**, 35079 (2019).
20. X. Bu, D. Okazaki, and S. Ashihara, Opt. Express **30**, 8517 (2022).
21. S. Vasilyev, M. Goma, I. Moskalev, *et al.*, in *CLEO: Science and Innovations* (2024), paper SM1H.4.
22. T. H. Wu, L. Ledezma, C. Fredrick, *et al.*, Nat. Photonics **18**, 218 (2024).
23. M. Kowalczyk, N. Nagl, P. Steinleitner, *et al.*, Optica **10**, 801 (2023).
24. A. V. Muraviev, V. O. Smolski, Z. E. Loparo, *et al.*, Nat. Photonics **12**, 209 (2018).
25. A. V. Muraviev, D. Konnov, and K. L. Vodopyanov, Sci. Rep. **10**, 18700 (2020).
26. S. Ghimire, A. D. DiChiara, E. Sistrunk, *et al.*, Nat. Phys. **7**, 138 (2011).
27. G. Vampa, S. Vasilyev, H. Liu, *et al.*, Opt. Lett. **44**, 259 (2019).